THE JOURNAL OF PHYSICAL CHEMISTRY C

Article

pubs.acs.org/JPCC

Theoretical Study of the Adsorption/Dissociation Reactions of Formic Acid on the α-Al_2O_3(0001) Surface

Min Ruan,[†,‡] Hua Hou,[†] Wen Li,*[,‡] and Baoshan Wang*[,†]

[†]College of Chemistry and Molecular Science, Wuhan University, Wuhan, China

[‡]Hubei Key Laboratory of Mine Environmental Pollution Control & Remediation, Hubei Polytechnic University, Huangshi, Hubei, China

Supporting Information

ABSTRACT: Formic acid was used as the model of lauric acid to investigate the microscopic mechanism of the anti-icing behavior and was checked to find out if it can be catalyzed to produce H_2 for fuel cells by the α-Al_2O_3(0001) 2 × 2 supercell slab model. The density functional theory with the all-electron double numerical polarized basis sets was employed. The results show that when it involves the carboxyl O and hydroxyl H atom the 1,2-dissociated adsorbate is the most stable intermediate on the dry Al_2O_3(0001) surface and is energetic barrier free to form the fairly stable ROCO- and HO-covered surface with the binding energy of 59.5 kcal/mol, and this dissociation mode has the lowest energy barrier of 14.9 kcal/mol to form the HOCO- and H_2O-covered surface after the surface is fully hydroxylated. The energetic barrier of the HCOOH dehydrogenation and dehydration reactions on the alumina surface decreased considerably from 65.3 to 30.6 kcal/mol and from 62.1 to 26.8 kcal/mol, respectively, in comparison with the gaseous decomposition. The dissociated configuration of lauric acid was tested, and it was found that it dissociated with free energy barrier through 1,2-hydrogen migration into the $C_{11}H_{23}OCO$- and HO-covered surface with a binding energy of 60.7 kcal/mol. The present theoretical work is useful to gain some new insights on the microscopic interaction mechanism of the superhydrophobic alumina surface fabrication procedure and on the heterogeneous catalysis reactions of the H_2 production.

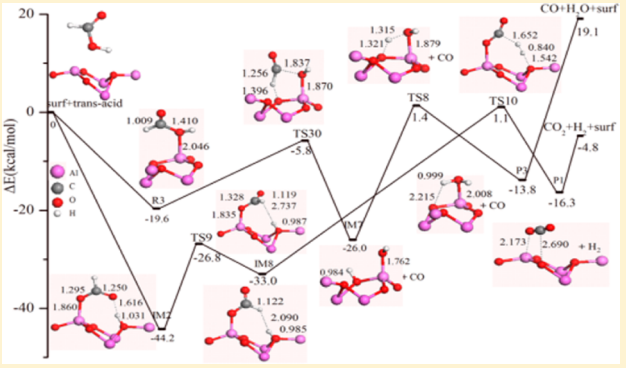

1. INTRODUCTION

The production of H_2 is a great challenge in heterogeneous catalysis. The decompositions of several carbon-containing compounds such as methanol, ethanol, and dimethyl ether are used as sources of H_2.[1−4] As the simplest and the most abundant fatty acid,[5] formic acid is the potential source of H_2 for fuel cells.[6]

Metal oxide is currently used for several applications of technological interest as a consequence of its electrical behavior and catalytic activity.[7−11] A focus of such exploration is the interfacial interaction of the highly valuable surface.[12−16] Alumina is used extensively as a substrate for heterogeneous catalysis.[17] Among the many polymorphs of alumina, the thermodynamically stable α-Al_2O_3, or corundum, has been studied most extensively, both experimentally and theoretically.[18−21]

Ojeda et al.[22] found that formic acid can form H_2 at high chemical potentials with the catalysis of Au on the Al_2O_3 surface. The adsorption of acetate species (CH_3COO^-) on the Ag/Al_2O_3 catalysis was studied by Gao et al.[23] Solymosi et al.[1] studied the dehydration of formic acid which was favored on the Au-deposited Al_2O_3 surface, and pure CO-free H_2 was obtained on Au/SiO_2 and Au/CeO_2 surfaces at below 473 K. However, the role of supporter Al_2O_3 in this reaction is unknown. Carlos-Cuellar et al.[24] investigated the heterogeneous uptake kinetics of formaldehyde on α-Al_2O_3 with a Knudsen cell reactor at 295 K. Tong et al.[25] studied the atmospheric heterogeneous reactions of formic acid on dust particles (Al_2O_3) at ambient conditions by using a DRIFTS reactor and found that the carboxylates had formed during the uptake process.

Additionally, we have obtained the superhydrophobic alumina surface with anti-icing property by etching with chemicals and modifying with low-surface energetic subject fatty acid,[26,27] but the reaction mechanism between the surface and fatty acid is unknown. In order to understand more about the anti-icing behavior of the superhydrophobic surface, the microscopic adsorption/dissociation mechanisms of fatty acid on the alumina surface should be investigated. Formic acid is used as the model of fatty acid to reveal the reaction mechanisms on the α-Al_2O_3(0001) surface. Furthermore, the catalytic mechanisms of dehydrogenation/dehydration reac-

Received: May 8, 2014
Revised: August 6, 2014
Published: August 15, 2014

dx.doi.org/10.1021/jp504542n | J. Phys. Chem. C 2014, 118, 20889−20898

tions of formic acid on the α-Al_2O_3(0001) surface are studied using the first-principles calculation based on density functional theory.

2. COMPUTATIONAL METHOD

For the slab calculation, we applied periodic, density-functional theoretical (DFT) calculations implemented in the Dmol^3 program.[28] To accurately account for the van der Waals (vdW) interactions, self-consistent field (SCF) energies of the systems were corrected for dispersion forces using the DFT-D3 method developed by Grimme et al.[29] The Kohn−Sham equation was solved in a self-consistent manner under the generalized gradient approximation (GGA).[30] Electron exchange and correlation energies were calculated using Becke−Lee−Yang−Parr (BLYP) with the all-electron double numerical (DND) and triple numerical polarized (TNP) basis sets.[31,32] DND basis sets include a d-type polarized function on heavy atoms, while the TNP basis sets include additional sets of d-type polarized functions on all atoms. The numerical basis set solving the atomic DFT equation is capable of minimizing or even eliminating basis set superposition error (BSSE).[33]

The atom-centered grids were used for the numerical integration with a real-space cutoff of 4.2 Å. The self-consistent-field (SCF) convergence criterion was set to the root-mean-square change in the electronic density to be less than 10^{-5} eV without thermal smearing. The equilibrium geometries of reactants, intermediates, and products were fully optimized using the Broyden Flecher Goldfarb Shanno (BFGS) method within the delocalized coordinates. Transition states were obtained tentatively using the synchronous transit methods and then refined through the eigenvector following optimization. The convergence criteria applied for geometry optimization were enforced to 2×10^{-5} au for energy, 0.004 au/Å for force, and 0.005 Å for maximum displacement. Harmonic vibrational frequencies of the optimized structures were computed by diagonalizing the mass-weighted second-derivative matrix which was built using two-sided finite differences with a displacement step of 0.01 Å and with HessianAtoms sets of relaxed atoms.

The Al-terminated α-Al_2O_3(0001) basal surface was built by cleaving the bulk corundum crystal whose lattice constants were a = 4.759 Å and c = 12.991 Å. It consisted of an 18-layer-thick slab with six complete AlO_3Al layers ($Al_{12}O_{18}$). To avoid unphysical interlayer interactions, the slabs were separated by a vacuum region of 10 Å. The BLYP/DND with Γ-point calculation was performed with a 2 × 2 supercell model ($Al_{48}O_{72}$) in this work. In all calculations, we allowed the top five atomic layers of the slab and their adsorbates to relax, whereas the other 13 atomic layers were held fixed at the bulk positions. In this work, we calculated the adsorption energies according to the following equation, $E_{ads} = E(\text{slab + adsorbate}) - E(\text{slab}) - E(\text{adsorbate})$, in which E(slab + adsorbate), E(slab), and E(adsorbate) were the calculated electronic energies of species adsorbed on the surface, the bare surface, and the gas-phase molecule, respectively.

3. RESULTS AND DISCUSSION

3.1. α-Al_2O_3(0001) 2 × 2 Supercell Surface Energy. The BLYP/DND with Γ-point calculations are performed with a 2 × 2 supercell bulk model ($Al_{48}O_{72}$) with the lattice constants of a = 9.518 Å and c = 12.991 Å and the $Al_{48}O_{72}$(0001) surface with the experimental lattice constants of a = 9.518 Å and c = 22.506 Å. The surface Al atoms relaxed toward the surface O atoms, decreasing the interlay spacing from 0.840 to 0.176 Å. The changes of the $Al_{48}O_{72}$(0001) surface before and after being optimized are shown as Figure 1. The relaxation ratio is

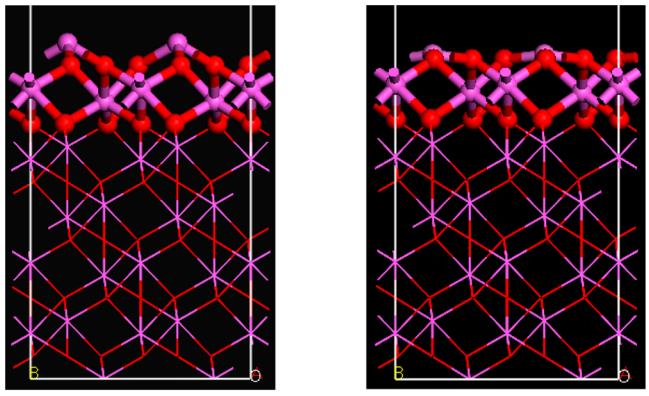

(a) before optimized (b) after optimized

Figure 1. Changes of the α-Al_2O_3(0001) surface before and after being optimized. The pink and red balls represent Al and O atoms, respectively.

79% in comparison with the experimental data of 51−63%.[34,35] The geometric reconstruction of the surface can be better characterized using the O−Al−O bond angle and the AlO_3 tetrahedral. The O−Al−O bond angle increases from 101.1° in the bulk to 118.9° in the surface, and the AlO_3 tetrahedral increases from 103.8° to 159.6°. The relaxation ratio is 17.6% and 53.8%, respectively. The surface energy is 1.70 J/m^2 (SE = $(E_{surface} - E_{bulk})/2A$, where A is the basal surface area) which is nearly the same as the experimental value of 1.69 J/m^2.[36] We know that the four Al atoms on the surface have the same chemical surrounding, which means that they have the same reactive site as a Lewis acid from the figure.

3. 2. Free HCOOH Molecule. In the gas phase, the isolated HCOOH molecule has cis and trans conformations, and it prefers the trans position.[37] The trans is 4.7 kcal/mol more stable than the cis at the theoretical level of BLYP/DND/1 × 1 × 1 in this study, as other studies[38,39] depicted. The bond distances and bond angles of the optimized *trans*-HCOOH structure are depicted in Table 1. Our results obtained from the table agree well with experiment[38] and with previously published DFT results.[39]

Table 1. Bond Distances (Å) and Bond Angles (deg) for the Gas-Phase *trans*-HCOOH

	C−O	C═O	C−H	O−H	O−C−O	C−O−H
this paper	1.367	1.212	1.104	0.992	125.3	105.9
experiment[a]	1.361	1.217	1.106	0.984	123.4	107.3
calculation[b]	1.356	1.206	1.108	0.982	124.9	106.1

[a]From ref 38. [b]From ref 39.

3.3. Theoretical Level. Table 2 shows the influences of basis sets, k-point mesh, atomic orbital cutoff value, and vacuum thickness on the binding energy of adsorbed compound IM1 (optimized geometry is shown in Figure 2). The binding energy is 59.5 kcal/mol at the theoretical level of BLYP/DND/1 × 1 × 1 with the atomic orbital cutoff value of 4.2 Å and the vacuum thickness of 10 Å. If the k-point is changed to be 3 × 3 × 3, the

dx.doi.org/10.1021/jp504542n | J. Phys. Chem. C 2014, 118, 20889−20898

Table 2. Adsorption Energies of IM1 at Different Theoretical Levels (kcal/mol)

effect factor	adsorption energies at different theoretical levels					
basis set	DND	DND	DND	DNP	TNP	DND
k-point	1 × 1 × 1	3 × 3 × 3	1 × 1 × 1	1 × 1 × 1	1 × 1 × 1	1 × 1 × 1
cutoff (Å)	4.2	4.2	4.8	4.2	4.2	4.2
vacuum thickness (Å)	10	10	10	10	10	20
ΔE^a(kcal/mol)	−59.5	−58.1	−56.2	−57.2	−59.6	−57.7

[a]Relative energies to the isolated formic acid and the free α-Al_2O_3(0001) surface.

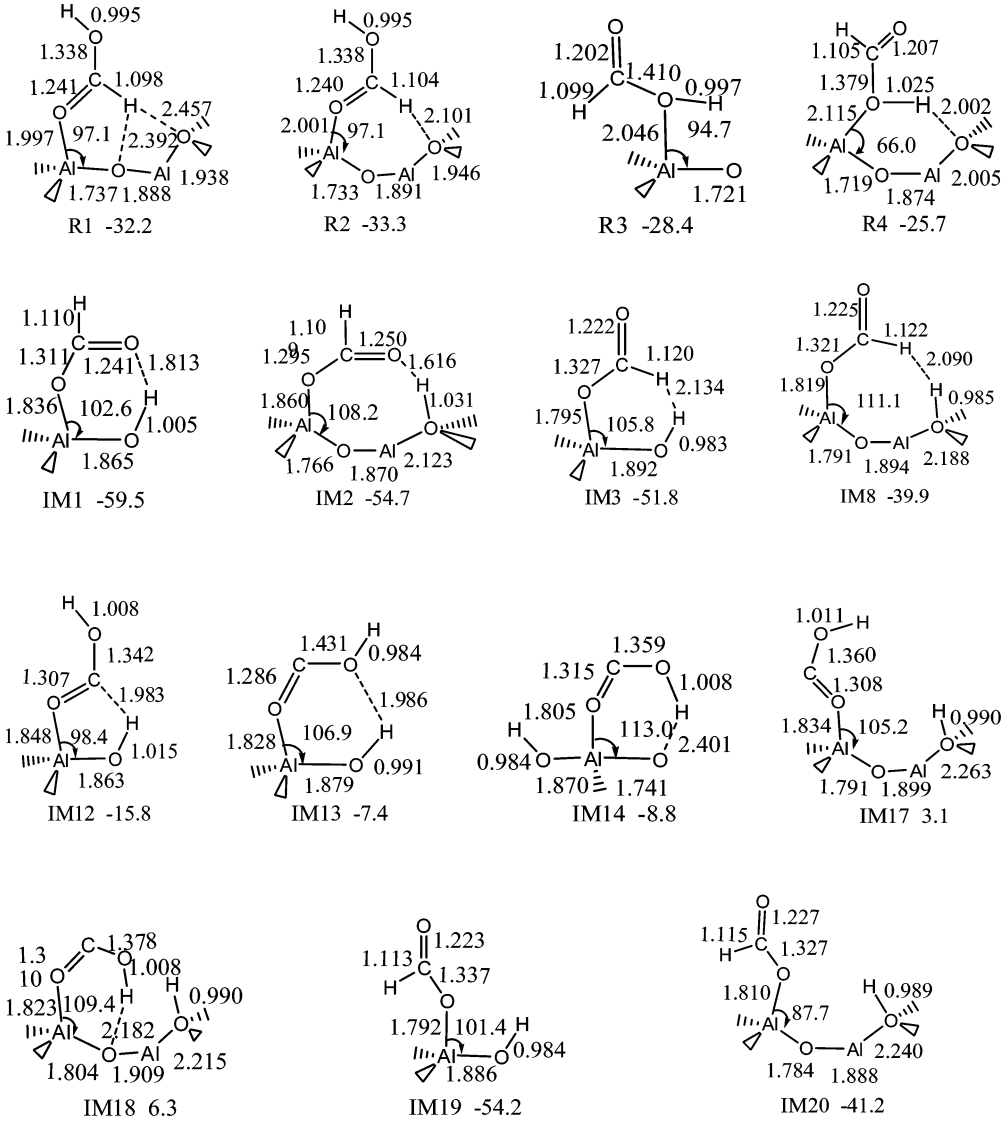

Figure 2. Geometries of the adsorption structures of formic acid on the α-Al_2O_3(0001) surface. Bond distances are in angstroms, and angles are in degrees.

binding energy is 58.1 kcal/mol. If the atomic orbital cutoff value is changed to be 4.8 Å, the binding energy is 56.2 kcal/mol. The value is 57.2 and 59.6 kcal/mol with the basis sets being changed to be DNP and TNP, respectively. The binding energy is 57.7 kcal/mol with changing vacuum thickness of 20 Å. From the above results, it can be concluded that the influences of basis sets, k-point mesh, vacuum region, and atomic orbital cutoff value have little significance on the research system. All calculations are performed at the theoretical level of BLYP/DND/1 × 1 × 1 with the atomic orbital cutoff of 4.2 Å and vacuum thickness of 10 Å.

Additionally, in order to certificate the model of the relaxed top five layers is proper in this work, we compare the energetic barrier of the reaction from R1 to IM12, TS16 (optimized geometries are shown in Figure S1, Supporting Information), with the relaxed top five-layer model and the relaxed top nine-layer model. They are calculated to be 24.3 and 26.7 kcal/mol, respectively. So the relaxation of the top five layers works well in this study.

3.4. Single HCOOH Adsorption/Dissociation at the 2 × 2 Supercell. A single isolated HCOOH molecule in all models with no restrictions can approach the α-Al_2O_3(0001)

dx.doi.org/10.1021/jp504542n | J. Phys. Chem. C 2014, 118, 20889−20898

surface to form two types of physical adsorbates, namely, carboxyl adsorption and hydroxyl adsorption, including R1, R2 and R3, R4, respectively, and to form one type of chemical dissociated adsorbate, including IM1 and IM2, two kinds of dissociated compounds. Their optimized geometries are shown in Figure 2. Their binding energies are 32.2, 33.3, 28.4, 25.7, 59.5, and 54.7 kcal/mol, respectively, as shown in Table S (Supporting Information) (E_{ads} = E(slab + adsorbate) − E(slab) − E(adsorbate), E(slab + adsorbate), E(slab), and E(adsorbate) are the energies of the adsorption compounds on the surface, the bare Al_2O_3(0001) surface, and the free formic acid molecule, respectively).

In the molecular adsorption compounds R1 and R2 of the carbonyl type, formic acid interacts with the surface through the carboxyl oxygen and the CH hydrogen. If the CH hydrogen atom locates at the 2-O_s (the nearest crystal oxygen to the Al atom) to form a five-membered ring, the binding energy of R1 is 32.2 kcal/mol. If the H atom locates at the 4-O_s (the second nearest crystal oxygen to the Al atom) to form a seven-membered ring, the binding energy of R2 is 33.3 kcal/mol. For the hydroxyl type adsorption compounds R3 and R4, the main interactions involve the hydroxyl O atom and H atom of formic acid. It forms an intermolecular four-membered ring of the hydroxyl H with the 2-O_s in R3, and it is a six-membered ring of the hydroxyl H with the 4-O_s in R4. The binding energy of R3 and R4 is 28.4 and 25.7 kcal/mol, respectively. Among the molecular adsorbates, R2 is the most stable complex.

If the formic acid approaches the surface through the carboxyl O atom and hydroxyl H atom, it can dissociate into HCOO and H without overcoming any energetic barrier. If the dissociated H atom interacts with the 2-O_s atom, the intermediate is IM1 with a six-membered ring. If the dissociated H atom interacts with the 4-O_s atom, the intermediate is IM2 with an eight-membered ring. The binding energy of IM1 and IM2 is 59.5 and 54.7 kcal/mol, respectively. To certificate the energetic barrier free process of this kind of dissociation, we fixed the C═O and O−H bonds of formic acid, scanned the Al_s−O_f bond length, and optimized the geometries of the molecular adsorption compounds. The adsorption energies of the compounds along the Al_s−O_f bond lengths are shown in Figure 3. We can see that the binding energies are increasing

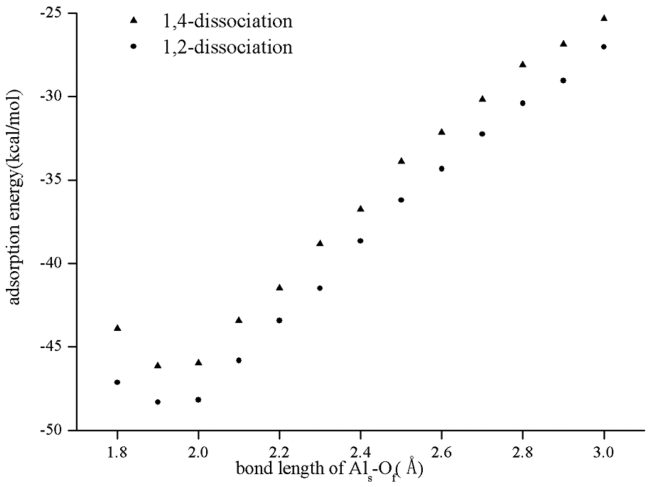

Figure 3. Adsorption energetic changes with formic acid approaching the α-Al_2O_3(0001) surface through the carboxyl O atom and hydroxyl H atom. Bond distances are in angstroms, and angles are in degrees.

along with formic acid approaching the surface until it reaches 1.9 Å, the bond length of the Al−O bond. This confirms the above result that it is free-barrier energetic dissociation when interactions involve carboxyl O and hydroxyl H.

The geometric changes after formic acid adsorption/dissociation at the 2 × 2 supercell α-Al_2O_3(0001) surface are listed in Table 3. As depicted, the bond length of Al_s−O_f is between 1.997 and 2.115 Å for the physical adsorption compounds R1, R2, R3, and R4. For the dissociated compounds, the bond length of Al_s−O_f is 1.836 and 1.860 Å in IM1 and IM2, respectively, and there is a new bond O_s−H_f with the length of 1.005 and 1.031 Å in IM1 and IM2, respectively. The adsorption/dissociation of formic acid can draw up the surface Al_s atom, as shown by d_{Al-O} which is the distance of the outmost Al_s to the next nearest O_s. The d_{Al-O} increases from 0.176 to 0.470, 0.456, 0.375, 0.421, 0.554, and 0.593 Å for R1, R2, R3, R4, IM1, and IM2 complexes, respectively. Obviously, the dissociation intermediates can draw up the Al atom more than the adsorption compounds, and R1 and R2 can draw up a little more than R3 and R4. We note that this bond length of Al_s−O_s in IM1 is 1.869 Å which is even 0.113 Å longer than that in the bulk of 1.856 Å. The $O_sAl_sO_s$ bond angle and the Al_sO_{s3} tetrahedral of the outmost layer of the surface decrease as the Al_s atom is drawn up. They decrease about 6° and 28° for the carbonyl adsorbates, about 4° and 21° for the hydroxyl adsorbates, and about 14° and 40° for the dissociated intermediates, respectively. In the dissociated intermediate IM1, the angle and tetrahedral is close to that in the bulk, and they are 104.8° and 119.2° in IM1 and 101.1° and 103.8° in the bulk.

There are four dissociation pathways for the four molecular adsorption compounds. The adsorption energies are shown in Table S (Supporting Information), and the optimized geometries are shown in Figure S1 (Supporting Information). The dissociated intermediations are COOH and H for the carbonyl adsorbates. The first route, starting from the initial molecular adduct of R1, possesses a five-membered ring transition state, TS16. The hydrogen atom migrates from formic acid to the 2-O_s to form the 1,2-dissociated intermediate IM12 with the binding energy of 15.8 kcal/mol. The barrier height for TS16 is 24.3 kcal/mol. In the second dissociation path, the hydrogen atom migrates from formic acid to the 4-O_s through TS25 to form the 1,4-dissociated intermediate IM17 with the exothermicity of 3.1 kcal/mol, and the barrier height for TS25 is as high as 54.5 kcal/mol. Obviously, for the carbonyl adsorbates, the 1,2-dissociation is easier than the 1,4-dissociation, and the 1,2-dissociated intermediate IM12 is 18.9 kcal/mol more stable than the 1,4-dissociated intermediate IM17. The dissociated intermediations are HCOO and H for the hydroxyl adsorbates in the later two pathways. If the route starts from R3, it possesses a four-membered ring transition state, TS31, with the energetic barrier of 15.0 kcal/mol to form the 1,2-dissociated intermediate IM19 with the binding energy of 54.2 kcal/mol. If the route starts from R4, it possesses a six-membered ring transition state, TS36, with the energetic barrier of 7.2 kcal/mol to form the 1,4-dissociation intermediate IM20 with the binding energy of 41.2 kcal/mol. The 1,2-dissociated intermediate IM19 is 13.0 kcal/mol more stable than the 1,4-dissociated intermediate IM20. The dissociated intermediate HCOO of the hydroxyl adsorbates is about 56.2 kcal/mol more stable than that of the carbonyl adsorbates when they adsorb on the α-Al_2O_3(0001) surface. Through overcoming 2.4 and 1.7 kcal/mol energetic barriers, the HCOO group in IM19 and

dx.doi.org/10.1021/jp504542n | J. Phys. Chem. C 2014, 118, 20889−20898

Table 3. Geometric Changes after Formic Acid Adsorption/Dissociation at the α-Al_2O_3(0001) Surface

model	O_s-H_f[a]	Al_s-O_f[b]	d_{Al-O}[c]	$\delta(d_{Al-O})$	l_{Al-O}[d]	$\delta(l_{Al-O})$	A_{OAlO}[e]	$\delta(A_{OAlO})$	$\varphi(AlO_3)$[f]	$\delta(\varphi_{AlO3})$
bulk			0.840		1.856		101.1		103.8	
surf			0.176		1.703		118.9		159.6	
R1	2.392	1.997	0.470	0.294	1.737	0.034	112.6	−6.3	131.2	−28.4
R2	2.101	2.001	0.456	0.280	1.733	0.030	112.1	−6.8	131.9	−27.7
R3	2.650	2.046	0.375	0.199	1.719	0.016	114.5	−4.4	139.3	−20.3
R4	1.983	2.103	0.421	0.245	1.721	0.018	115.2	−3.7	137.2	−22.4
IM1	1.005	1.836	0.554	0.378	1.869	0.166	104.8	−14.1	119.2	−40.4
IM2	1.031	1.860	0.593	0.417	1.766	0.063	105.9	−13.0	119.5	−40.1

[a]The bond distance of the outmost O_s atom of the surface and the H_f atom of formic acid, in angstroms. [b]The bond distance of the outmost Al_s atom of the surface and the O_f atom of formic acid, in angstroms. [c]Interlayer spacing between the outmost Al_s and O_s layers, in angstroms, and δ represents the changes before and after formic acid adsorption on the clean surface. [d]Al_s-O_s bond distance of the outmost layer on the surface, in angstroms. [e]Bond angle of the $O_sAl_sO_s$ of the outmost layer on the surface, in angstroms. [f]Dihedral angle of the Al_sO_{s3} tetrahedral structure, in degrees.

IM20 can rotate to form IM3 and IM8 with the adsorption energies of 51.8 and 39.9 kcal/mol, respectively. The COOH group in IM12 can rotate to IM13 and IM14 and in IM17 can rotate to IM18. The COOH group in IM12 is the most stable formation.

We study the vibrational properties of IM1 since it is the most stable intermediate. An IR spectrum of the isolated formic acid molecule is necessary. It is difficult to find the spectrum of an isolated formic acid molecule in the gas phase experimentally because it is mainly found as a dimer in the atmosphere.[40] However, formic acid monomers have been studied in an argon matrix at low temperatures and low pressures.[41] Therefore, theoretical calculations are useful to validate previous experimental work. As shown in Table 4, the calculated

Table 4. Calculated Vibrational Frequencies (in cm^{-1}) of the Gas-Phase Formic Acid and of the Adsorption Complexes at the 2 × 2 Supercell Al_2O_3(0001) Surface at the BLYP/DND Level

modes[a]	formic acid	formic acid[b]	R3	IM1	IM1[c]
$\nu(O_fH_f)$	3512	3570	3497	-	-
$\nu(O_sH)$	-	-	-	3184	-
$\nu(CH_f)$	2936	2944	3039	2885	2866
$\nu(C{=}O_f)$	1754	1776	1775	-	-
$\nu_{as}(O_fCO_f)$	-	-	-	1608	1600
$\delta(CH_f)$	1356	-	1378	1373	1378
$\delta(O_fH)$	1268	1223	1205	-	-
$\delta(O_sH)$	-	-	-	1263	-
$\nu_s(O_fCO_f)$	-	-	-	1266	1393
$\nu(C-O_f)$	1054	1105	976	-	-

[a]as = asymmetric mode, s = symmetric mode, ν = stretching, δ = bending in-plane. [b]In the gas phase.[28] [c]Experimental data in parentheses taken from ref 25.

frequencies for the isolated formic acid molecule are in good agreement with the experimental values, an indication of the good quality of the theoretical data. At the same time, we can get the molecular frequencies of the adsorbed compounds as R3 on the Al_2O_3 surface that cannot be observed in experiments.

The O_fH_f stretching frequencies, $\nu(O_fH_f)$, of the isolated formic acid are calculated at 3512 cm^{-1} which disappears in IM1 because the H atom migrates from formic acid to the 2-O_s atom. Instead, there is a new band at 3184 cm^{-1}, which corresponds to the stretching vibrational mode of the O_s-H_f bond. The IR spectrum of the physical adsorption compound cannot be recorded experimentally, but we can see that from the frequency calculations. There is a 15 cm^{-1} low-frequency shift of the $\nu(O_fH_f)$ in R3, owing to the direct interaction between O_f and Al_s which weakens the O_f-H_f bond. The $C-H_f$ stretching vibration of IM1 has a red shift of 51 to 2885 cm^{-1} which is similar to the experiments of ref 25 of 2866 cm^{-1} after the dissociation at the surface; on the contrary, a high-frequency shift of 113 cm^{-1} is observed in the $\nu(CH_f)$ mode in R3. The reaction of formic acid on the surface to give the formate anion is suggested by the absence of the $C{=}O_f$ stretch mode at 1780 cm^{-1} and the $C-O_fH_f$ stretch mode at 1100 cm^{-1}.[42] The $C{=}O_f$ stretch mode is at 1754 cm^{-1} in formic acid and at 1775 cm^{-1} in R3, and the $C-O_fH_f$ stretch mode is at 1054 cm^{-1} in formic acid and at 976 cm^{-1} in R3; however, they disappear in IM1. Instead, we see the asymmetric and symmetric stretch modes of O_fCO_f at 1608 and 1266 cm^{-1} in IM1, respectively. The wavenumber of the O_fCO_f asymmetric stretch mode is very satisfied with the experimental data 1600 cm^{-1} which was studied by Tong et al.,[25] but that for the symmetric mode is smaller than the experimental value of 1393 cm^{-1}. The bending in-plane $\delta(CH_f)$ mode has about a 25 cm^{-1} high-frequency shift in both R3 and IM1 compared to the free HCOOH molecule, and it is nearly the same as that in ref 25 of 1378 cm^{-1}. The bending in-plane $\delta(O_fH)$ disappears in IM1, and it is replaced by $\delta(O_sH)$ with the vibrational frequencies at 1263 cm^{-1}. The $\delta(O_fH)$ has a 63 cm^{-1} low-frequency shift to 1205 cm^{-1} in R3 after being adsorbed on surface. The IR spectra confirmed that the molecular frequencies of the most stable intermediate IM1 are satisfied with the experiments.

3.5. HCOOH Dehydrogenation/Dehydration at the 2 × 2 Supercell. Furthermore, we studied the dehydrogenation and dehydration of HCOOH on the 2 × 2 supercell α-Al_2O_3(0001) surface. The optimized geometries and the adsorption energies for all of the reactants, intermediates, transition states, and products are shown in Figure S1 and Table S (Supporting Information), respectively. All of the energetic routes are shown in Figures S2−4(Supporting Information). Figure 4 gives the predominant energetic routes. For the predominant dehydrogenation route, if the free formic acid molecule approaches the α-Al_2O_3(0001) surface without any constraints through the carboxyl O atom and hydroxyl H atom, the O−H bond of formic acid dissociates through an energetic barrier free process to form IM2 with binding energy of 54.7 kcal/mol first. Then the formate(HCOO) overcomes an energetic barrier of 19.1 kcal/mol to form IM8 with the

dx.doi.org/10.1021/jp504542n | J. Phys. Chem. C 2014, 118, 20889−20898

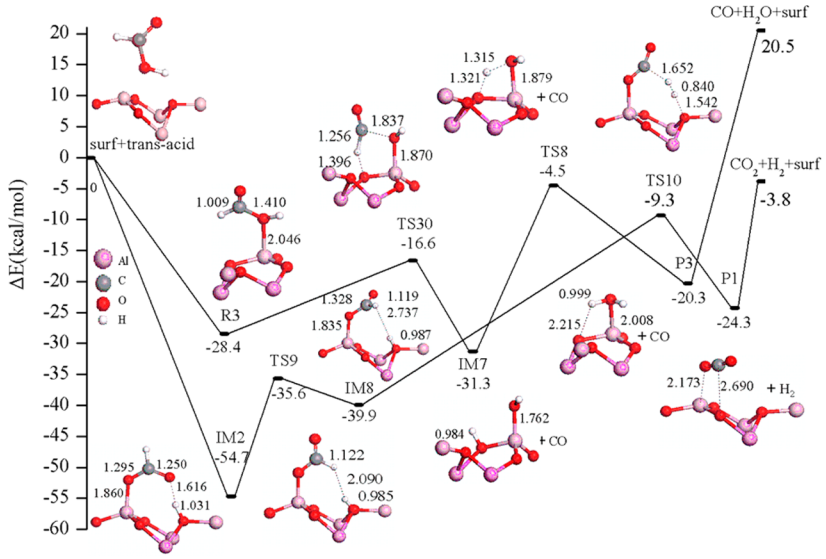

Figure 4. Predominant energetic routes for the dehydrogenation and dehydration reactions of formic acid on the α-Al_2O_3(0001) surface.

Table 5. Energetic Barrier of Dehydration/Dehydrogenation of Formic Acid (kcal/mol)

method	dehydrogenation	dehydration
experiment[43]	65−68	62−65
experiment[44]	48.5	60.5
PMP4/6-311++G(d,p)//UMP2/6-311G(d,p)[45]	65.2	63.0
B3LYP/6-311+G(2d,p)//HF/3-21G(d,p)[46]	67.8	66.8
MP2/6-311G//HF/6-311G[47]	77.6	67.1
B3LYP/6-311G(2d,p)// MP2/6-311G(2d,p)[48]	73.3	56.0
in the gas phase in this work	65.3	62.1
on the α-Al_2O_3(0001) surface in this work	30.6	26.8

binding energy of 39.9 kcal/mol. In IM8, the CH hydrogen and hydroxyl H are in the distance of 2.090 Å.

Then, IM8 overcomes the 30.6 kcal/mol energetic barrier to break the C−H bond to produce H_2 away from the surface and CO_2 adsorbing on the surface with the binding energy of 24.3 kcal/mol through TS10. In TS10, the C−H and O_s−H bond lengths increase from 1.122 and 0.985 Å to 1.652 and 1.542 Å, respectively, and the distance between the two H atoms decreases from 2.090 to 0.840 Å. The O and C atom of CO_2 is in the distance of 2.173 and 2.690 Å with the surface Al and O atom, respectively. The energy of free CO_2 and H_2 molecules compared with that of the free HCOOH molecule is −3.8 kcal/mol; that is, the dehydrogenation reaction of formic acid on the α-Al_2O_3(0001) surface is slightly exothermic by 3.8 kcal/mol. The C−H bond breaking step is the rate-determining step of the dehydrogenation reaction of formic acid on the α-Al_2O_3(0001) surface with the energetic barrier of 30.6 kcal/mol. Other experimental and theoretical energetic barriers for the dehydrogenation and dehydration reactions of formic acid are shown in Table 5. The energetic barrier of the dehydrogenation reaction of formic acid in the gas phase with our model is 65.3 kcal/mol in this work, and it is the same as the experiment[43] of 65−68 kcal/mol; however, it is different from the experimental[44] value of of 48.5 kcal/mol which is tested at the low voltage of 0.03−0.3 atm, and it is consistent with the calculated value of 65.2 kcal/mol at the level of PMP4/6-311++G(d,p)//UMP2/6-311G(d,p)[45] and of 67.8 kcal/mol at the level of B3LYP/6-311+G(2d,p)//HF/3-21G(d,p).[46] The values at the level of MP2/6-311G//HF/6-311G[47] and B3LYP/6-311G(2d,p)//MP2/6-311G(2d,p)[48] are 77.6 and 73.3 kcal/mol, respectively. It can be seen that the dehydrogenation of formic acid on the α-Al_2O_3(0001) surface can be enhanced considerably with the energetic barrier decreasing from 65.3 to 30.6 kcal/mol.

The dehydration reaction path starts from R3 whose C−O and C−H bonds break simultaneously through the five-membered ring transition state TS30 with the energetic barrier of 11.8 kcal/mol to form IM7 with binding energy of 31.3 kcal/mol. In TS30, the C−H and C−O bond lengths increase from 1.009 and 1.410 Å to 1.256 and 1.837 Å, respectively, and the distance between CH hydrogen and the 2-O_s is 1.396 Å. In IM17, the CO free molecule runs away from the α-Al_2O_3(0001) surface, and the dissociated OH and H bond with the surface Al atom and 2-O_s atom with the bond length of 1.762 and 0.984 Å, respectively. Then the H atom transfers from the 2-O_s atom to the hydroxyl O atom through the four-membered ring transition state TS8 with an energetic barrier of 26.8 kcal/mol to form the adsorbed H_2O molecule with the binding energy of 20.3 kcal/mol. In TS8, the migrating H atom is almost in the middle of the two O atoms with the distances of O−H bonds 1.321 and 1.315 Å, respectively. The bond length between the O atom of the adsorbed H_2O molecule and the surface Al atom is 2.008 Å. The energy of free CO and H_2O molecules compared with the free HCOOH molecule is 20.5 kcal/mol; that is, the dehydration reaction of formic acid on the α-Al_2O_3(0001) surface is endothermic by 20.5 kcal/mol. The rate-determining step of the dehydration reaction of formic acid on the Al_2O_3 surface is the forming of the O−H bond in the water molecule with the energetic barrier of 26.8 kcal/mol. The energetic barrier of the dehydration reaction of formic acid in

dx.doi.org/10.1021/jp504542n | J. Phys. Chem. C 2014, 118, 20889−20898

the gas phase is 62.1 kcal/mol with our model in this work, and it is nearly the same as the experimental values of 62−65 kcal/mol[43] and of 60.5 kcal/mol[44] and is consistent with other calculations.[45−48] It can be seen that the dehydration of formic acid on the α-Al_2O_3(0001) can be enhanced considerably with the energetic barrier decreasing from 62.1 to 26.8 kcal/mol.

3.6. Two HCOOH Molecule Adsorption at the 2 × 2 Supercell. Since the surface Al atom can bond with more than one O atom, it is interesting to investigate how the second HCOOH or more HCOOH molecules react with the α-Al_2O_3(0001) surface. Starting from the most stable structure of the molecular adsorbed compound R1, one formic acid molecule attacks the surface Al atom to form compound R5 with a weak bond, as shown in Figure 5. The Al_s-O_f bond is

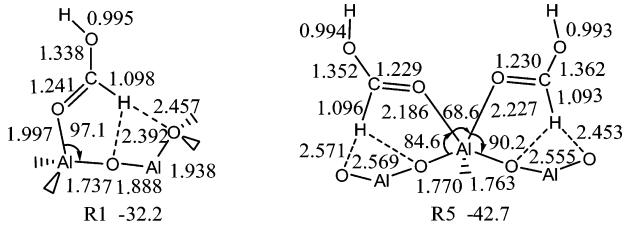

Figure 5. Adsorption intermediates formed by addition of one/two HCOOH molecules to the α-Al_2O_3(0001) surface.

relatively long, 2.186 and 2.227 Å, compared with the bond length of 1.997 Å in R1. The C−O bond of formic acid increases from 1.338 to 1.352 Å and 1.362 Å, respectively. The second formic acid can draw up the Al atom since the distance between the first layer Al atoms and the first layer O atoms is 0.7 Å in R5 compared with that of 0.4 Å in R1. Meanwhile, the $O_s-Al_s-O_f$ angle decreased from 97.1° to 90.2° and 84.6°, respectively, and the $O_f-Al_s-O_f$ bond angle between the two HCOOH molecules is 68.6°. The binding energy of R5 is 42.7 kcal/mol, which is slightly larger than that of R1, 32.2 kcal/mol. The two formic acid molecules can absorb stably on the same surface Al atom through carboxyl O atoms, but they cannot bond with the same Al atom after dissociating into HCOO and H. It concludes that each surface Al atom can just bond with one dissociated HCOOH molecule.

3.7. Fully Hydroxylated 2 × 2 Supercell Surface. Hydroxylation of the metal oxide surface is a general issue, and it is important to analyze the influence of hydroxyl groups on the reaction of formic acid at the α-Al_2O_3(0001) surface.

The coordinatively unsaturated surface Al ions provide strong Lewis acid (electron-acceptor) sites for H_2O adsorption.[49] It is believed that water dissociates on the Al-terminated Al_2O_3(0001) surface, and the mechanism of water at the Al_2O_3(0001) surface has been calculated extensively using various cluster/lattice models and first-principles methodologies.[50−56] Wittbrodt et al.[57] employed three cluster models to investigate the interaction of water with the (0001) surface of α-Al_2O_3 at the B3LYP/6-31+G* level of theory. It was found that there are two types of dissociative reactions; namely, 1−2 (proton transfer to the nearest crystal oxygen) and 1−4 (proton transfer to the second nearest oxygen) addition of water take place. Wang et al.[58] studied a single water molecular dissociation model on the α-Al_2O_3(0001) surface at the BLYP/TNP/3 × 3 × 3 k-points level of theory and found that in the 2 × 2 supercell model the hydroxylation prefers 1,2-dissociation which is exothermic by 37.3 kcal/mol. The author also calculated the multiple layer adsorption and confirmed that the outmost Al atom of the (0001) surface is hydroxylated by one H_2O molecule and inert to further hydroxylation by water.

Accordingly, the fully hydroxylated Al_2O_3(0001) 2 × 2 supercell surface with the outmost four Al atoms being hydroxylated by $4H_2O$ molecules through the 1,2-migration mode was studied in this work, and the geometry of the surface is shown in Figure 6. The dissociated OH bonds with Al atom,

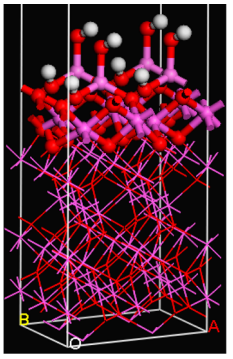

Figure 6. Optimized slab model of the hydroxylated α-Al_2O_3(0001) 2 × 2 supercell surface.

and the H atom bonds with the surface O atom, forming a new layer. The geometric and energetic changes from the clean to the fully hydroxylated 2 × 2 supercell Al_2O_3(0001) surface are listed in Table 6. It is obvious that the dissociation adsorption of water draws up the surface Al atoms. The distance of the surface Al to the first oxygen plane is increased by 0.408 Å. The bond length of Al−O of the outmost layer increases to 1.862 Å which is a little longer than that of the bulk. The bond angle of OAlO and the dihedral angle of the AlO_3 tetrahedral decrease 14.1° and 48.4°, respectively, after the surface is hydroxylated fully by the water molecule.

The adsorption energy for $4H_2O$ molecules dissociation at the α-Al_2O_3(0001) 2 × 2 supercell surface is −166.7 kcal/mol, namely, −41.4 kcal/mol for each H_2O molecule dissociation on the surface. The calculated energy in the work compares well to the experimental values of −23 to −41 kcal/mol.[59]

3.8. HCOOH Adsorption at the Fully Hydroxylated 2 × 2 Supercell. The optimized geometries of the formic acid molecule at the hydroxylated 2 × 2 supercell Al_2O_3(0001) surface are shown in Figure 7. The O and H atoms of formic acid interact with the hydroxylated O−H hydrogen and Al−OH oxygen of the surface, respectively, in the physical adsorption compounds. When formic acid interacts with the surface through hydroxyl O and H atoms, it forms R1 with the binding energy of 22.7 kcal/mol. In the molecular adsorption compounds R2 (O atom reacts with the 4-H of surface OH) and R3 (O atom reacts with the 2-H of surface OH), formic acid interacts with the surface through the carboxyl oxygen and the OH hydrogen with the binding energy 21.4 and 25.3 kcal/mol, respectively. When the main interactions involve the hydroxyl O atom and CH hydrogen atom, it forms R4 with the binding energy of 11.1 kcal/mol. When it invovles the carboxyl O atom and CH hydrogen atom, it forms R5 with the binding energy of 19.6 kcal/mol.

Considering the O−H bond dissociation of formic acid into P1 and P2 with the binding energy of 24.5 and 27.4 kcal/mol, the product HCOO and H_2O molecule react with the same surface Al atom through an oxygen atom.

dx.doi.org/10.1021/jp504542n | J. Phys. Chem. C 2014, 118, 20889−20898

Table 6. Geometric and Energetic Changes from the Clean to the Hydroxylated 2 × 2 Supercell α-$Al_2O_3(0001)$ Surface

model	d_{Al-O}	$\delta(d_{Al-O})$	l_{Al-O}	$\delta(l_{Al-O})$	A_{OAlO}	$\delta(A_{OAlO})$	$\varphi(AlO_3)$	$\delta(\varphi_{AlO3})$	E_{ads}
bulk	0.840		1.856		101.1		103.8		
clean surface	0.176		1.703		118.9		159.6		
hydroxylation	0.584	0.408	1.862	0.159	104.8	−14.1	111.2	−48.4	−166.7

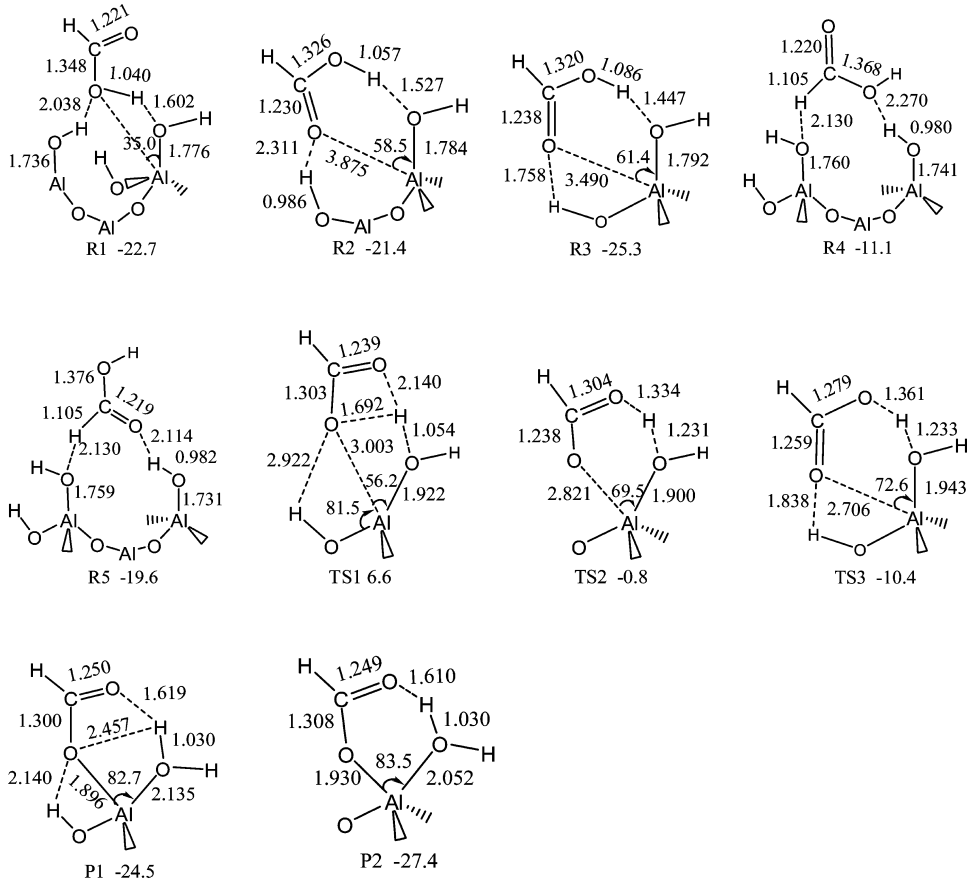

Figure 7. Optimized geometries and adsorption energies of the formic acid molecule at the fully hydroxylated α-$Al_2O_3(0001)$ 2 × 2 supercell surface. Bond distances are in angstroms, and energies are in kcal/mol.

When it starts from R1, the product forms through the four-membered ring transition state TS1 with the energy barrier of 29.3 kcal/mol. If the reactors are R2 and R3, they overcome a 19.6 and 14.9 kcal/mol energy barrier through a six-membered ring transition state, respectively.

This can conclude that the prominent route for HCOOH dissociation at the fully hydroxylated α-$Al_2O_3(0001)$ 2 × 2 supercell surface is starting from R3 that through the 1,2-site adsorbs on the surface to form the HOCO−Al−OH_2 covered surface. The energy barrier is 14.9 kcal/mol, and the binding energy of the product is 24.5 kcal/mol. So it is easier for formic acid to dissociate at the dry α-$Al_2O_3(0001)$ surface which is energy barrier free.

3.8. Lauric Acid Dissociation at the 2 × 2 Supercell. In order to study the superhydrophobic mechanism of the α-Al_2O_3 surface modified with lauric acid, the absorption/dissociation of formic acid at the α-$Al_2O_3(0001)$ 2 × 2 supercell surface was studied as the model. The optimized geometries are shown in Figure 8. This confirms that the most stable intermediate of the HCOOH molecule is the 1,2-dissociated intermediate involving the carboxyl O and hydroxyl H with the binding energy of 59.5 kcal/mol. In order to testify the dissociation configuration of lauric acid, the geometries of the free $C_{11}H_{23}COOH$ molecule and the dissociated intermediate were studied. It was found that the lauric acid molecule dissociated into $C_{11}H_{23}OCO$- and HO-covered surface, and it was energy barrier free with the binding energy of 60.7 kcal/mol. It can be seen that the superhydrophobic alkylation group spread upward which contributes the superhydrophobicity of the alumina surface.

4. CONCLUSIONS

The formic acid molecule is adsorbed on the outer Al sites of the α-$Al_2O_3(0001)$ surface by two approaches, namely, carbonyl adsorption and hydroxyl absorption. The molecular adsorption compound involving the carboxyl O atom and CH hydrogen with the surface 4-O_s is the most stable one with the binding energy of 33.3 kcal/mol. The chemical dissociation via either 1,2- or 1,4-hydrogen migration is a free energetic barrier when it involves the carboxyl O and hydroxyl H atoms, and the 1,2-dissociation produces the most stable intermediate with the binding energy of 59.5 kcal/mol. When the modifier lauric acid dissociates on the alumina surface, it forms the stable $C_{11}H_{23}OCO$- and HO-covered surfaces with the binding energy of 60.7 kcal/mol.

dx.doi.org/10.1021/jp504542n | J. Phys. Chem. C 2014, 118, 20889−20898

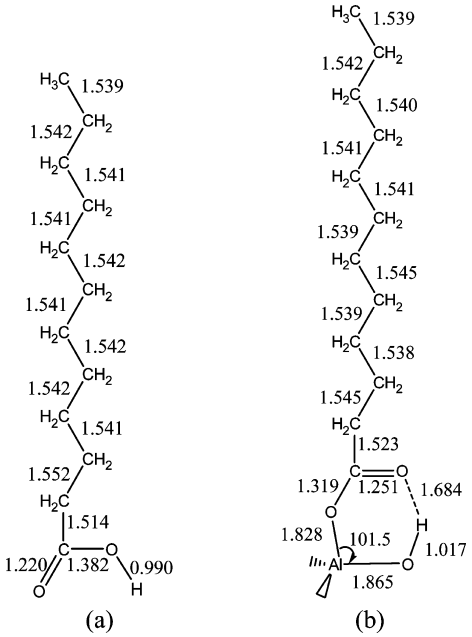

Figure 8. Optimized geometries of the free lauric acid molecule (a) and the 1,2-dissociated intermediate (b) at the α-Al_2O_3(0001) 2 × 2 supercell surface.

As for the vibrational frequencies, we can calculate those of the dissociated intermediates and the molecular adsorption compounds which cannot be observed in experiments on the α-Al_2O_3(0001) surface. The O_f–H_f and C=O_f stretching vibrations disappear in the dissociated intermediate compared to the free formic acid at 1754 cm^{-1} and molecular adsorbed compound at 1775 cm^{-1}, but two new vibrational modes are attributed as the ν_{as}(OCO) and ν_s(OCO) at 1608 and 1266 cm^{-1}, respectively. The bending in-plane δ(C–H_f) in the molecular compound at 1378 cm^{-1} is the same as that in the dissociated intermediates at 1373 cm^{-1}. These values are consistent with experiments and confirm that the most stable intermediate is the 1,2-dissociated intermediate involving the carboxyl O and hydroxyl H.

Dehydrogenation and dehydration routes have been revealed theoretically on the α-Al_2O_3(0001) surfaces. The predominant reaction path to form CO_2 + H_2 proceeds via the stepwise mechanisms with the energetic barrier of 30.6 kcal/mol. In contrast, the formation of CO + H_2O involves the concerted CO and CH bond breaking with the energetic barrier of 26.8 kcal/mol. In comparison with the gaseous unimolecular decomposition of formic acid, the energetic barrier of the dehydrogenation and dehydration reaction can be decreased 34.7 and 35.3 kcal/mol by the α-Al_2O_3(0001) surface.

Furthermore, two formic acid molecules are considered to be stable to adsorb physically on the same surface Al atom as indicated by the calculated binding energy of 42.7 kcal/mol, but just one dissociated HCOOH molecule can bond with each surface Al atom.

The influence of the hydroxylation on the dissociation of formic acid at the α-Al_2O_3(0001) surface is analyzed. It finds that the 1,2-dissociation involving the carboxyl O atom and OH hydrogen has the lowest energy barrier of 14.9 kcal/mol to form HOCO- and H_2O-covered surfaces.

The dissociated configuration of lauric acid at the α-Al_2O_3(0001) surface is tested. It can dissociated into $C_{11}H_{23}OCO$- and HO-covered surfaces with the binding energy of 60.7 kcal/mol and free energy barrier.

■ ASSOCIATED CONTENT

Supporting Information

Table S and Figures S1–S4. This material is available free of charge via the Internet at http://pubs.acs.org.

■ AUTHOR INFORMATION

Corresponding Authors

*E-mail: baoshan@whu.edu.cn. Phone: (86)27-6875-6347.
*E-mail: wenl@ualberta.ca. Phone: 780-492-1652.

Notes

The authors declare no competing financial interest.

■ ACKNOWLEDGMENTS

This work was financially supported by the NSFC (21273166, 51272082, 21174047), the Major Program of Education Bureau of Hubei Province, China (Z20104401), the Provincial Key Program of Natural Science Foundation of Hubei Province, China (2010CDA026).

■ REFERENCES

(1) Gazsi, A.; Bánsági, T.; Solymosi, F. Decomposition and Reforming of Formic Acid on Supported Au Catalysts: Production of CO-Free H_2. *J. Phys. Chem. C* **2011**, *115*, 15459–15466.
(2) Gazsi, A.; Bánsági, T.; Solymosi, F. Hydrogen Formation in the Reactions of Methanol on Supported Au Catalysts. *Catal. Lett.* **2009**, *131*, 33–41.
(3) Gazsi, A.; Koós, Á.; Bánsági, T.; Solymosi, F. Adsorption and Decomposition of Ethanol on Supported Au Catalysts. *Catal. Today.* **2011**, *160*, 70–78.
(4) Gazsi, A.; Ugrai, I.; Solymosi, F. Production of Hydrogen from Dimethyl Ether on Supported Au Catalysts. *Appl. Catal., A* **2011**, *391*, 360–366.
(5) Barteau, M. A. Site Requirements of Reactions on Oxide Surfaces. *J. Vac. Sci. Technol., A* **1993**, *11*, 2162–2168.
(6) Choi, J. H.; Jeong, K. J.; Dong, Y.; Han, J.; Lim, T. H.; Lee, J. S.; Sung, Y. E. Electro-Oxidation of Methanol and Formic Acid on PtRu and PtAu for Direct Liquid Fuel Cells. *J. Power Sources.* **2006**, *163*, 71–75.
(7) Henrich, V. E. The Surfaces of Metal Oxides. *Rep. Prog. Phys.* **1985**, *48*, 1481–1541.
(8) Freund, H. J. Adsorption of Gases on Solid Surfaces. *Ber. Bunsen-Ges. Phys. Chem.* **1995**, *99*, 1261–1281.
(9) Henrich, V. E.; Cox, P. A. *The Surface Science of Metal Oxides*; Cambridge: England, 1996.
(10) Freund, H. J.; Kuhlenbeck, H.; Staemmler, V. Oxide Surfaces. *Rep. Prog. Phys.* **1996**, *59*, 283–347.
(11) Freund, H. J. Adsorption of Gases on Complex Solid Surfaces. *Angew. Chem., Int. Ed. Engl.* **1997**, *36*, 452–475.
(12) Ertl, G.; Knoezinger, H.; Weitkamp, J. *Handbook of Heterogeneous Catalysis*; VCH: Weinheim, Germany, 1997.
(13) Campbell, C. T. Ultrathin Metal Films and Particles on Oxide Surfaces: Structural, Electronic and Chemisorptive Properties. *Surf. Sci. Rep.* **1997**, *27*, 1–111.
(14) Haruta, M. Size- and Support-Dependency in the Datalysis of Gold. *Catal. Today.* **1997**, *36*, 153–166.
(15) Henry, C. R. Surface Studies of Supported Model Catalysts. *Surf. Sci. Rep.* **1998**, *31*, 231–235.
(16) Bäumer, M.; Freund, H. J. Metal Deposits on Well-Ordered Oxide Films. *Prog. Surf. Sci.* **1999**, *61*, 127–198.
(17) Eng, P. J.; Trainor, T. P.; Brown, G. B.; Waychunas, G. A.; Newville, M.; Sutton, S. R.; Rivers, M. L. Structure of the Hydrated α-Al_2O_3(0001) Surface. *Science.* **2000**, *288*, 1029–1033.

(18) Yao, N.; Wang, Z. L.; Cowley, J. M. REM and REELS Identifications of Atomic Terminations at α-Alumina (011) Surface. *Surf. Sci.* **1989**, *208*, 533−549.
(19) Wefers, K.; Misra, C. *Oxides and hydroxides of Aluminum Alcoa Technical Paper*; Alcoa Laboratories: Michigan, 1987.
(20) Levin, I.; Brandon, D. Alumina Polymorphs: Crystal Structures and Transition Sequences. *J. Am. Ceram. Soc.* **1998**, *81*, 1995−2012.
(21) Zheng, L. Q.; Li, Z. R.; Bourdo, S.; Khedir, K. R.; Asar, M. P.; Ryerson, C. C. Exceptional Superhydrophobicity and Low Velocity Impact Icephobicity of Acetone- Functionalized Carbon Nanotube Films. *Langmuir* **2011**, *27*, 9936−9943.
(22) Ojeda, M.; Iglesia, E. Formic Acid Dehydrogenation on Au-Based Catalysts at Near-Ambient Temperatures. *Angew. Chem., Int. Ed.* **2009**, *48*, 4800−4803.
(23) Gao, H. W.; Yan, T. X.; Yu, Y. B.; He, H. DFT and DRIFTS Studies on the Adsorption of Acetate on the Ag/Al_2O_3 Catalyst. *J. Phys. Chem. C* **2008**, *112*, 6933−6938.
(24) Carlos-Cuellar, S.; Li, P.; Christensen, A. P.; Krueger, B. J.; Burrichter, C.; Grassian, V. H. Heterogeneous Uptake Kinetics of Volatile Organic Compounds on Oxide Surfaces Using a Knudsen Cell Reactor: Adsorption of Acetic Acid, Formaldehyde, and Methanol on α-Fe_2O_3, α-Al_2O_3, and SiO_2. *J. Phys. Chem. A* **2003**, *107*, 4250−4261.
(25) Tong, S. R.; Wu, L. Y.; Ge, M. F.; Wang, W. G.; Pu, Z. F. Heterogeneous Chemistry of Monocarboxylic Acids on α-Al_2O_3 at Different Relative Humidities. *Atmos. Chem. Phys.* **2010**, *10*, 7561−7574.
(26) Ruan, M.; Li, W.; Wang, B. S.; Deng, B. W.; Ma, F. M.; Yu, Z. L. Fabrication and Anti-Icing Behavior of Superhydrophobic Surfaces on Aluminum Alloy Substrates. *Langmuir* **2013**, *29*, 8482−8491.
(27) Ruan, M.; Li, W.; Wang, B. S.; Luo, Q.; Ma, F. M.; Yu, Z. L. Optimal Conditions for the Preparation of Superhydrophobic Surfaces on Al Substrates Using a Simple Etching Approach. *Appl. Surf. Sci.* **2012**, *258*, 7031−7035.
(28) Delley, B. From Molecules to Solids with the DMol3 Approach. *J. Chem. Phys.* **2000**, *113*, 7756−7764.
(29) Grimme, S.; Antony, J.; Ehrlich, S.; Krieg, H. A Consistent and Accurate Ab Initio Parametrization of Density Functional Dispersion Correction (DFT-D) for the 94 Elements H-Pu. *J. Chem. Phys.* **2010**, *132*, 154104−154123.
(30) White, J. A.; Bird, D. M. Implementation of Gradient-Corrected Exchange- Correlation Potentials in Car-Parrinello Total-Energy Calculations. *Phys. Rev. B* **1994**, *50*, 4954−4957.
(31) Becke, A. D. A multicenter Numerical Integration Scheme for Polyatomic Molecules. *J. Chem. Phys.* **1988**, *88*, 2547−2553.
(32) Lee, C. T.; Yang, W. T.; Parr, R. G. Development of the Colle-Salvetti Correlation- Energy Formula into a Functional of the Electron Density. *Phys. Rev. B* **1988**, *37*, 785−789.
(33) Inada, Y.; Orita, H. Efficiency of Numerical Basis Sets for Predicting the Binding Energies of Hydrogen Bonded Complexes: Evidence of Small Basis Set Superposition Error Compared to Gaussian Basis Sets. *J. Comput. Chem.* **2008**, *29*, 225−232.
(34) Guenard, P.; Renaud, G.; Barbier, A.; Gautier-Soyer, M. Determination of the α-Al_2O_3(0001) Surface Relaxation and Termination by Measurements of Crystal Truncation Rods. *Surf. Rev. Lett.* **1998**, *5*, 321−324.
(35) Ahn, J.; Rabalais, J. W. Composition and Structure of the Al_2O_3{0001}-(1 × 1) Surface. *Surf. Sci.* **1997**, *388*, 121−131.
(36) McHale, J. M.; Navrotsky, A.; Perrotta, A. J. Effects of Increased Surface Area and Chemisorbed H_2O on the Relative Stability of Nanocrystalline γ-Al_2O_3 and α-Al_2O_3. *J. Phys. Chem. B* **1997**, *101*, 603−613.
(37) Vittadini, A.; Selloni, A.; Rotzinger, F. P.; Grätzel, M. Formic Acid Adsorption on Dry and Hydrated TiO_2 Anatase (101) Surfaces by DFT Calculations. *J. Phys. Chem. B* **2000**, *104*, 1300−1306.
(38) Almenningen, A.; Bastiansen, O.; Motzfeldt, T. A Reinvestigation of the Structure of Monomer and Dimer Formic Acid by Gas Electron Diffraction Technique. *Acta Chem. Scand.* **1969**, *23*, 2848.
(39) Szymanski, M. S.; Gillan, M. J. The Energetics of Adsorption of HCOOH on the MgO(100) Surface. *J. Surf. Sci.* **1996**, *367*, 135−148.
(40) Jolly, G. S.; McKenney, D. J.; Singleton, D. L.; Paraskevopoulos, G.; Bossard, A. R. Rates of Hydroxyl Radical Reactions. Part 14. Rate Constant and Mechanism for the Reaction of Hydroxyl Radical with Formic Acid. *J. Phys. Chem.* **1986**, *90*, 6557−6562.
(41) Reva, I. D.; Plokhotnichenko, A. M.; Radchenko, E. D.; Sheina, G. G.; Blagoi, Yu. P. The IR Spectrum of Formic Acid in an Argon Matrix. *Spectrochim. Acta A* **1994**, *50*, 1107−1111.
(42) Klein, J.; Léger, A.; Belin, M.; Défourneau, D.; Sangster, M. J. L. Inelastic- Electron-Tunneling Spectroscopy of Metal-Insulator-Metal Junctions. *Phys. Rev. B* **1973**, *7*, 2336−2348.
(43) Hsu, D. S. Y.; Shaub, W. M.; Blackburn, M.; Lin, M. C. Kinetic Modeling of CO Production from the Reaction of CH_3 with O-2 in Shock-Waves. *Ber. Bunsen-Ges. Phys. Chem.* **1983**, *87*, 909−2348.
(44) Blake, P. G.; Davies, H. H.; Jackson, G. E. Dehydration Mechanisms in the Thermal Decomposition of Gaseous Formic Acid. *J. Chem. Soc. B* **1971**, 1923−1925.
(45) Francisco, J. S. A Comprehensive Theoretical Examination of Primary Dissociation Pathways of Formic Acid. *J. Chem. Phys.* **1992**, *96*, 1167−1992.
(46) Akiya, N.; Savage, P. E. Role of Water in Formic Acid Decomposition. *AIChE J.* **1998**, *44*, 405−415.
(47) Ruelle, P.; Kesselring, U. W.; Nam-Tran, H. Ab Initio Quantum-Chemical Study of the Unimolecular Pyrolysis Mechanisms of Formic Acid. *J. Am. Chem. Soc.* **1986**, *108*, 371−375.
(48) Yagasaki, T.; Saito, S.; Ohmine, I. A Theoretical Study on Decomposition of Formic Acid in Sub- and Supercritical Water. *J. Chem. Phys.* **2002**, *117*, 7631−7639.
(49) Hass, K. C.; Schneider, W. F.; Curioni, A.; Andreoni, W. The Chemistry of Water on Alumina Surfaces: Reaction Dynamics from First Principles. *Science* **1998**, *282*, 265−268.
(50) Polly, R.; Schimmelpfennig, B.; Florsheimer, M.; Kruse, K.; Monem, A.; Klenze, R.; Rauhut, G.; Fanghanel, T. Theoretical Investigation of the Water/Corundum (0001) Interface. *J. Chem. Phys.* **2009**, *130*, 064702.
(51) Fernandez, E. M.; Eglitis, R.; Borstel, G.; Balbas, L. C. Ab Initio Calculations of H_2O and O-2 Adsorption on Al_2O_3 Substrates. *Comput. Mater. Sci.* **2007**, *39*, 587−592.
(52) Wang, X. G.; Chaka, A.; Schefer, M. Effect of the Environment on α-Al2O3 (0001) Surface Structures. *Phys. Rev. Lett.* **2000**, *84*, 3650−3653.
(53) Shapovalov, V.; Truong, T. N. Ab Initio Study of Water Adsorption on α-Al_2O_3 (0001) Crystal Surface. *J. Phys. Chem. B* **2000**, *104*, 9859−9863.
(54) Lodziana, Z.; Norskov, J. K.; Stoltze, P. The stability of the Hydroxylated (0001) Surface of Alpha-Al_2O_3. *J. Chem. Phys.* **2003**, *118*, 11179−11188.
(55) De Leeuw, N. H.; Parker, S. C. Effect of Chemisorption and Physisorption of Water on the Surface Structure and Stability of Alpha-alumina. *J. Am. Ceram. Soc.* **1999**, *82*, 3209−3216.
(56) Thissen, P.; Grundmeier, G.; Wippermann, S.; Schmidt, W. G. Water Adsorption on the Alpha-Al_2O_3(0001) Surface. *Phys. Rev. B* **2009**, *80*, 245403.
(57) Wittbrodt, J. M.; Hase, W. L.; Schlegel, H. B. Ab Initio Study of the Interaction of Water with Cluster Models of the Aluminum Terminated (0001) α-Aluminum Oxide Surface. *J. Phys. Chem. B* **1998**, *102*, 6539−6548.
(58) Wang, B. S.; Hou, H.; Luo, Y. B.; Li, Y.; Zhao, Y. M.; Li, X. L. Density Functional/All-Electron Basis Set Slab Model Calculations of the Adsorption/ Dissociation Mechanisms of Water on α-Al_2O_3(0001) Surface. *J. Phys. Chem. C* **2011**, *115*, 13399−13411.
(59) Nelson, C. E.; Elam, J. W.; Cameron, M. A.; Tolbert, M. A.; George, S. M. Desorption of H_2O from a Hydroxylated Single-Crystal Alpha-Al_2O_3(0001) Surface. *Surf. Sci.* **1998**, *416*, 341−353.